Tacticity-Induced Changes in the Micellization and Degradation Properties of Poly(lactic acid)-block-poly(ethylene glycol) Copolymers

Cite as:
Agatemor, C., & Shaver, M. P. (2013). Tacticity-Induced Changes in the Micellization and Degradation Properties of Poly(lactic acid)-block-poly(ethylene glycol) Copolymers. *Biomacromolecules*, 14(3), 699-708.

Manuscript received: 20/11/2012; Accepted: 13/02/2013; Article published: 26/02/2013

Tacticity-induced Changes in the Micellization and Degradation Properties of Poly(lactic acid)-*block*-poly(ethylene glycol) Copolymers**

Christian Agatemor[1] and Michael P. Shaver[1,2,*]

[1]Department of Chemistry, University of Prince Edward Island, 550 University Avenue, Charlottetown, PE, C1A 4P3, Canada.

[2]EaStCHEM, School of Chemistry, Joseph Black Building, University of Edinburgh, West Mains Road, Edinburgh, EH9 3JJ, UK.

[*]Corresponding author; e-mail: michael.shaver@ed.ac.uk

[**]We acknowledge the financial support of the Natural Sciences and Engineering Research Council of Canada, the Canada Foundation for Innovation and the Atlantic Canada Opportunities Agency as well as support from the Universities of Prince Edward Island and Edinburgh. We also thank Drs. Rabin Bissessur and Brian Wagner, UPEI, for access to TGA, DSC and fluorescence instruments.

Supporting information:
Additional characterization data including GPC traces, DSC thermograms, and fluorescence plots for the copolymers are provided. This information is available free of charge via the Internet at http://pubs.acs.org/

Graphical abstract:

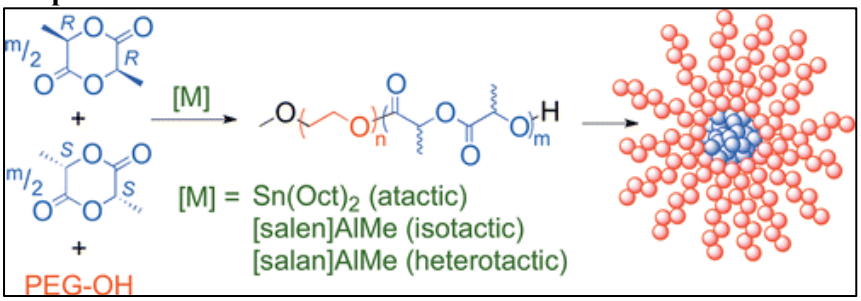

Keywords:
poly(lactic acid); poly(ethylene glycol); block copolymers; ring-opening polymerization; catalysis; tacticity; critical micelle concentration; degradation; thermal properties

Abstract

Poly(lactic acid)-*block*-poly(ethylene glycol) copolymers (PLA-*b*-PEG) featuring varying tacticities (atactic, heterotactic, isotactic) in the PLA block were synthesized and investigated for their micellar stability, degradation and thermal properties. Utilizing tin(II) bis(2-ethylhexanoate), aluminum salan and aluminum salen catalysts, the copolymers were synthesized through the ring-opening polymerization of d-, l-, *rac*- or a blend of l- and *rac*-lactide using monomethoxy-poly(ethylene glycol) as a macroinitiator. The critical micelle concentration, which reflects the micellar stability, was probed using a fluorescence spectroscopic method with pyrene as the probe. The copolymers were degraded in a methanolic solution of 1,5,7-triaza-bicyclo[4.4.0]dec-5-ene and the degradation was measured by ^{1}H NMR spectroscopic and gel permeation chromatographic analyses. Differential scanning calorimetry and thermogravimetric analysis provided information on the thermal properties of the copolymers. Atactic and heterotactic microstructures in the PLA block resulted in lower micellar stability, as well as faster degradation and shorter erosion time compared to polymers with high isotactic enchainment (P_m). By modification of the P_m, micellar stability, degradation and erosion rates of the copolymers can be tuned to specific biomedical applications. Interestingly, while tin(II) bis(2-ethylhexanoate) and aluminum salan-catalyzed PLA-*b*-PEG copolymers exhibited similar micellization behavior, the aluminum salen-catalyzed PLA-*b*-PEG exhibited unique behavior at high micelle concentration in the presence of the pyrene probe. This unique behavior can be attributed to the disintegration of the micelles through the interactions of long isotactic stereoblock segments.

Introduction

The design and biomedical applications of macromolecules are rapidly evolving, with contributions from synthetic chemistry, material science and biomedical engineering. Macromolecules such as polymersomes,[1] polymeric nanoparticles,[2] polymer-drug conjugates[3] polymeric hydrogels[4] and polymeric micelles and vesicles[5] have been engineered for controlled drug delivery, improved drug efficacy and safety, ameliorated drug physicochemical properties and enhanced pharmacokinetic profiles. Of great interest to macromolecular chemists are amphiphilic block copolymers that are capable of adopting various morphologies with an inner core for the encapsulation and storage of bioactives such as drugs.[5-7] In a selective solvent, polymeric amphiphiles can self-assemble into micelles that are characterized by a nanoscopic structure with a hydrophobic core and hydrophilic corona when the copolymer concentration in the solvent exceeds a threshold concentration known as the critical micelle concentration (CMC).

Functionally, the hydrophobic core acts as a depot for the solubilization of hydrophobic drugs, storage and protection of unstable lipophilic drugs and transport of these encapsulated bioactives to the targeted tissue where it is needed. The hydrophilic corona enhances micellar solubility and stability within physiological systems while minimizing cellular adhesion and protein adsorption on micelles.[8] The micelles are of a size above the threshold for renal clearance,[9] giving prolonged circulation time and an enhanced permeability and retention (EPR) effect. EPR leads to increased accumulation of the encapsulated bioactives in tissues with increased vascular permeability and impaired lymphatic drainage, including solid tumors and inflamed tissues.[8-10] These advantages make polymeric micelles promising systems for an array of biomedical applications especially in the delivery of cancer therapeutics.[8]

These features aside, several obstacles hinder the efficient utilization of micelles as drug delivery systems including low drug loading capacity, poor *in vivo* stability, insufficient cellular uptake and triggered cargo release.[6,10] Crucial to the performance of micelles as drug vectors is the micellar stability *in vivo*; following intravenous administration, instability results in the uncontrolled dissociation of the micelles with an eventual burst release of the encapsulated bioactive. A low CMC is usually associated with micelles that are stable enough to survive the *in vivo* diluting effect of blood circulation,[10] with the *in vivo* stability of micelles dependent on the thermal properties as well as the structure and electronics of the amphiphile.[7,11,12] Approaches explored in enhancing micellar stability include increasing the hydrophobicity of the hydrophobic block of the copolymer,[13] promoting covalent crosslinking,[14] hydrogen bonding,[15] electrostatic ionic[16] or π-π interactions[17] within the micellar core. The size and chemical nature of the hydrophobic block also play an important role in shaping micellar properties and drug loading capacity.[18,19]

One factor that has not been systematically studied in micellar tuning is polymer tacticity. We have shown that tacticity plays a significant role in the properties of macromolecular structures.[20,21] Specifically, a recent study highlighted the influence of PLA tacticity (isotactic vs atactic) on the micellization property of poly(N-(2-hydroxypropyl)-methacrylamide)-*block*-poly(lactic acid).[22] Furthermore, the packing/crystallinity of the hydrophobic block, which is related to tacticity, is acknowledged to control the size and shape of the resultant micelle.[23-26] In this work we seek to study the tacticity-micellar stability relationship of a polymeric micelle formed from a diblock copolymer, poly(lactic acid)-*block*-poly(ethylene glycol) (PLA-*b*-PEG), a biomacromolecule of significant interest in drug delivery.

Our first approach involved tuning the tacticity of the poly(lactic acid) (PLA) block of PLA-*b*-PEG by varying the monomer composition from 100% l-lactide to 0% l-lactide in a monomer blend of l-lactide and *rac*-lactide while using tin(II) bis(2-ethylhexanoate) (**A**, Figure 1) as the catalyst to generate a series of copolymers with varying isotactic enchainments (P_m). This series was complemented by amphiphilic copolymers prepared using aluminum catalysts, ^{tBu}[salen]AlMe, (**B**), where ^{tBu}[salen] is *N*,*N*′-ethylenebis(3,5-di(tert-butyl)salicylimine), ^{Cl}[salan]AlMe, (**C**), where ^{Cl}[salan] is *N*,*N*′-ethylenebis(benzyl)bis(3,5-dichlorosalicylamine) and ^{Ad}[salen]AlMe, (**D**), where ^{Ad}[salen] is *N*,*N*′-ethylenebis(3-adamantyl-5-methylsalicylimine) (Figure 1), which promote isotactic stereoblock (sb) PLA (**B** and **D**) and heterotactic PLA (**C**) from the ring-opening polymerization of *rac*-lactide.[27-29] Through this approach, we seek to systematically probe the effect of tacticity on the stability of micelles by studying their CMCs, thermal properties and hydrolytic degradation. While an elegant single-pot ring-opening polymerization (ROP) of *rac*-lactide with mPEG (M_n = 2000 Da) by blending different aluminum catalysts was recently reported,[30] our study represents the first synthesis and systematic investigation of PLA-*b*-PLA copolymer featuring either a sb-PLA or a completely heterotactic PLA block and the correlation of a wider array of microstructures with micellar properties including CMCs (Scheme 1). Given the relevance of physical properties such as glass transition temperature (T_g), melting temperature (T_m), thermal stability and degradation rates in the optimum performance of polymeric biomolecules in biomedical applications, we also examined these properties as a function of tacticity. To our knowledge, this is the first systematic investigation of the effect of stereocontrol on the micellar stability, T_g, T_m, thermal stability and degradation profiles of PLA-*b*-PEG copolymers.

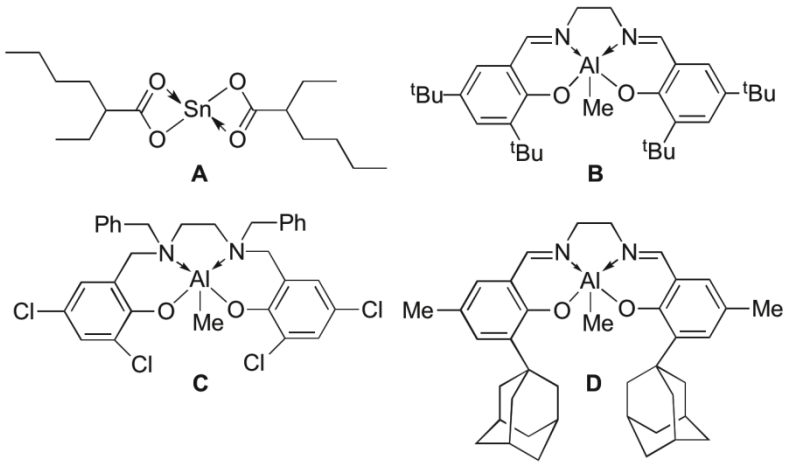

Figure 1. Catalysts employed for the ROP of lactide.

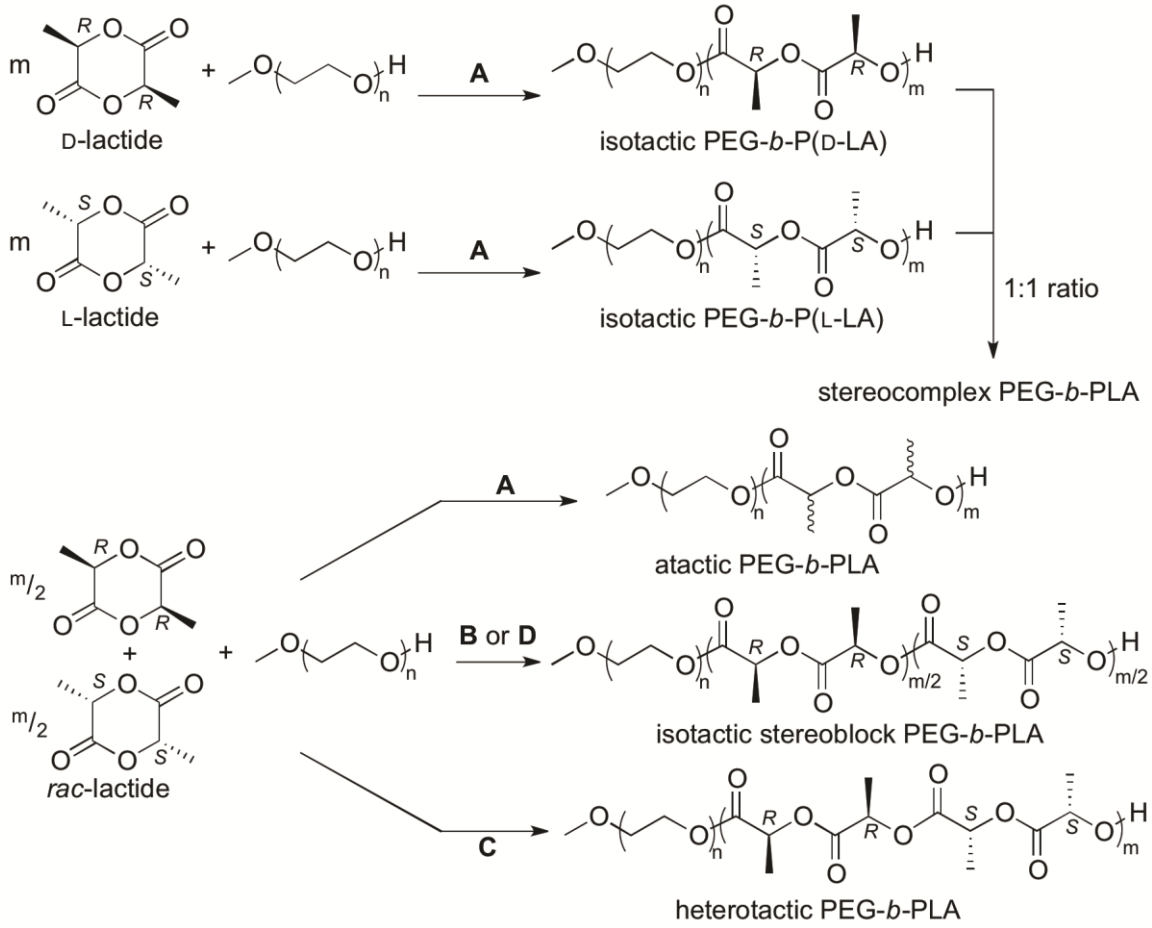

Scheme 1. PLA microstructures from the ROP of lactide in the presence of PEG initiator and the appropriate catalyst.

Experimental section

Materials. Monomethoxy poly(ethylene glycol) (mPEG) (M_n = 2000 Da) was obtained from Sigma-Aldrich (Canada) and dried as a solution in dry dichloromethane overnight over activated 3 Å molecular sieves. d-, l-, and *rac*-Lactide

were obtained from Purac Biomaterials (Netherlands) and were purified by three successive vacuum sublimations. Deuterated solvents were purchased from Cambridge Isotopes and either dried over 3 Å molecular sieves or CaH_2 (C_6D_6 and $CDCl_3$) and vacuum transferred prior to use. Tin(II) bis(2-ethylhexanoate) was purchased from Sigma-Aldrich (Canada) and purified by vacuum distillation. Trimethylaluminum (2.0 M solution in heptane), 2,4-dichlorophenol, *N,N'*-dibenzylethylenediamine, paraformaldehyde, 3,5-di-*tert*-butyl-2-hydroxybenzaldehyde, 1,2-diaminoethane, pyrene and 1,5,7-triazabicyclo[4,4,0]dec-5-ene, purchased from Sigma-Aldrich (Canada), were used without further purification. Toluene and n-pentane, obtained from Caledon Laboratories Ltd (Canada), were purified by passing the solvent through an Innovative Technologies solvent purification system that consisted of columns of alumina and copper catalyst, and were degassed thrice in a cycle of freeze-pump-thaw. Methanol and petroleum ether purchased from Sigma-Aldrich (Canada) and Caledon Laboratories Ltd (Canada), respectively, were used as received.

Synthesis. Synthetic experiments that involved air and moisture sensitive compounds were conducted in a nitrogen-filled MBraun LABmaster sp glovebox or in nitrogen-filled sealed ampoules. The syntheses of the aluminum catalysts (**B**-**D**) followed previously reported procedures.[27-29] The copolymers were synthesized via solution ROP of d-, l-, *rac*-lactide or a blend of *rac*- and l-lactide in the presence of the mPEG initiator and the appropriate catalyst (**A**-**D**). In a polymerization experiment, the monomer(s), mPEG and catalyst in a molar ratio of 23:1:1 and 5 mL of toluene were charged into an ampoule equipped with a magnetic stirrer bar in the glovebox. The ratio of the repeat unit in each block was arbitrarily chosen to be 1:1, as only the effect of tacticity was studied. The sealed ampoule was taken out of the glovebox and placed in a preheated oil bath maintained at 70 °C and the polymerization carried out until ≥98% monomer conversion was obtained. Monomer conversion was determined by means of ^{1}H NMR spectroscopy of the crude reaction mixture. Once the desired conversion was reached, the solution was cooled to room temperature, opened to the atmosphere and the copolymer precipitated from petroleum ether. The copolymers were dried in a vacuum oven maintained at 30 °C. For each different copolymer, two batches were prepared. Measurements were taken in triplicate. Deviations in molecular weight measurements between batches were less than 1% in all instances. For clarity, the results of only one batch are presented.

Instrumentation and characterization. A Bruker Avance NMR spectrometer (^{1}H, 300 MHz) was used to characterize the copolymers and catalysts in $CDCl_3$ or C_6D_6. The isotactic enchainment (P_m) was obtained from homonuclear decoupled ^{1}H NMR spectroscopy.[27,26,31] The spectra were acquired from a $CDCl_3$ solution of the copolymers with the methyl protons at δ 1.55 – 1.64 ppm decoupled from the methine proton at δ 5.15 – 5.25 ppm during the acquisition time. In an experiment, 16 scans were obtained with each scan consisting of 16,384 data points at a spectra width of 3591 Hz, pulse delay of 1 sec and a power level for decoupling of 30 dB. By taking the ratio of the integrated peak corresponding to the *iii* tetrad at δ 5.19 ppm to the entire methine region at δ 5.15 – 5.25 ppm, the P_m was obtained.[27,28]

Gel permeation chromatography (GPC) analyses were performed on a Polymer Laboratories PL-GPC 50 Plus integrated GPC system with two Jordi DVB mixed bed columns (300 x 7.5 mm) and absolute molecular weights were obtained using a refractive index detector coupled to a multiangle laser light scattering detector, the MiniDAWN Treos (Wyatt Technology, USA). GPC analyses were carried out in HPLC-grade THF (flow rate: 1 mL/min) at 50°C on samples of 1 mg/mL concentration. Differential scanning calorimetry (DSC) was conducted under nitrogen using a heat/cool/heat cycle at a heating rate of 5 °C/min on a TA Instruments DSC Q100 with aluminum pan while

thermogravimetric analysis (TGA) was performed in air at a heating rate of 10 °C/min on a TA Instruments TGA Q500 with platinum pan. Powder X-ray diffractograms (p-XRD) were acquired on a Bruker AXS Advanced D8 diffractometer equipped with a graphite monochromator, variable divergence, antiscatter slits and a scintillation detector. The diffractograms were obtained from fine powder of the copolymer adhered with double sided tape to a glass substrate and the experiment conducted under atmospheric conditions using a Cu Kα radiation (λ = 1.542 Å) and a scan range of 2 - 60°. The percent crystallinity (X_c) of copolymers was obtained via standard methods.[32]

Fluorescence spectroscopy. A standard fluorescence spectroscopy method[33-35] was used to determine the CMCs. Fluorescence spectra were obtained on a Photon Technology International (Canada) LS-100 luminescence spectrometer. A 2 mg/mL stock solution of copolymer micelles was obtained by dissolution of an appropriate mass of copolymer(s) in doubly distilled water (DDW) overnight.[33] Thereafter, 100 μL of 1.2 x 10^{-5} M pyrene stock solution was transferred to a 5 mL volumetric flask and an appropriate volume of a 2 mg/mL stock solution of the micelle and doubly distilled water were added to obtain the final polymer concentration. The final pyrene concentration in the working solutions for the fluorescence spectroscopy was 2.4 x 10^{-7} M. During fluorescence spectroscopic measurements, pyrene was excited at 334 nm and the intensities of the first (I_1) and third (I_3) vibrational bands were recorded. The copolymer concentration corresponding to a sharp increase in a plot of I_1 as a function of copolymer concentration and a sharp decrease in a plot of I_1/I_3 versus copolymer concentrations gave the CMC.[33-35]

Degradation studies. Following reported PLA degradation methodology,[20,21,36] a sample of the copolymer (200 mg) was pressed into pellets of uniform thickness and diameter under 2000 psi and suspended in 5.0 mL of methanolic solution of 1,5,7-triaza-bicyclo[4.4.0.]dec-5-ene (TBD) (0.05% w/v). The solution was left to stand at room temperature and the time required for complete erosion of the pellet was recorded. The solvent was evaporated at room temperature and the residue dissolved in $CDCl_3$ for ^{1}H NMR spectroscopy and in THF for GPC analyses to measure degradation.

Results and discussion

PLA-*block*-PEG Copolymers. Diblock copolymers of mPEG and PLA having an equal degree of polymerization for each block were prepared via the metal-catalyzed ring-opening polymerization of a stereomeric form of the lactide cyclic ester using monomethylated poly(ethylene glycol) (M_n = 2000 Da) as a macroinitiator. The first series of materials prepared exploited the tin-catalyzed ROP of l-lactide, *rac*-lactide and a blend of l- and *rac*-lactide to generate PLA-*b*-PEG materials. By varying the mole percent composition of l- and *rac*-lactide in the monomer blend, control was achieved over the product isospecificity, giving variable stereoregular enchainments, P_m (Sn-series, Table 1, entries 1-6). This series of polymers would necessarily contain long blocks of l-lactic acid with d-lactic acid stereoerrors. A complementary series of copolymers was prepared by the ROP of *rac*-lactide using mPEG (M_n = 2000 Da) as a macroinitiator and **B** or **C** as catalyst (Al-series, Table 1, Entries 7 and 8) producing isotactic stereoblock-PLA and heterotactic PLA blocks, respectively. Excellent control over the polymerizations was evidenced by the low polydispersity indices (PDIs) of the copolymers and good agreement between the theoretical number average molecular weight, $M_{n,th}$, and the M_n obtained from GPC and NMR analyses (Table 1). All of the copolymers were

synthesized to have similar M_n and PDI so as to minimize the effect of these properties on thermal behavior, degradation and self-assembly.

Table 1. Microstructural and polymerization data for PLA-*b*-PEG copolymers[a]

Entry	Conversion[b] (%)	Cat	Monomer (l:*rac*:d)	$M_{n,th}$	$M_{n,GPC}$[c]	M_w[c]	$M_{n,NMR}$[d]	PDI[c]	P_m[e]
1	100	**A**	100:0:0	5310	4500	5300	5280	1.20	1.00
2	99	**A**	80:20:0	5280	5300	6300	5380	1.20	0.84
3	99	**A**	60:40:0	5280	4400	5100	5300	1.20	0.54
4	99	**A**	40:60:0	5280	4900	5700	5310	1.20	0.46
5	99	**A**	20:80:0	5280	5200	6100	5350	1.20	0.39
6	98	**A**	0:100:0	5250	5100	5800	5320	1.10	0.34
7	100	**B**	0:100:0	5310	4500	5100	5100	1.10	0.80
8	100	**C**	0:100:0	5310	5000	5300	5370	1.10	0[f]

[a] Polymerization carried out at 70 °C in 5 mL toluene with monomer:initiator:catalyst ratio of 23:1:1. [b] Conversion obtained from ^{1}H NMR spectra. [c] M_n, M_w and PDI obtained from GPC analyses and rounded to the nearest 100 or 0.1 respectively. [d] M_n from ^{1}H NMR analyses [e] P_m, isotactic enchainment in the PLA block obtained from homonuclear decoupled ^{1}H NMR spectroscopy of the methine proton of the PLA block. [f] Heterotactic enchainment, $P_r = 0.94$.

In the Sn-series, the P_m was varied from 34-100% as determined from the homonuclear decoupled ^{1}H NMR spectra of the methine region of the PLA block. The tin-catalyzed ROP of lactide does not differentiate between the monomer diastereomers, producing random atactic PLA with *rac*-lactide and isotactic stereopure PLA with l-lactide[20,21,37] provided, in the latter case, there is no epimerization. This approach has previously been used to tune the P_m of PLA polymer stars to obtain PLA stars with isotacticity biases that decrease as the percent of l-lactide in the monomer blend decreases.[20] Catalyst **B** afforded a copolymer, **7**, with long, alternating blocks of l- and d-lactide to give a sb-PLA that had 80% isotactic enchainment, similar to the isotactic enchainment found in copolymer **2**. Structurally, the isotactic copolymers **2** and **7** thus differ significantly as the PLA block in **7** contains semi-crystalline stereoblocks of both poly(l-lactic acid) and poly(d-lactic acid) linked by short amorphous atactic stereoerrors while **2** is predominantly homochiral poly(l-lactic acid) with atactic segments from *rac*-lactide inclusion.[38] In linear and star macrostructures, these differences can lead to altered polymer properties, especially in their crystallinity.[20,21,37]

Thermal properties of copolymers. One of the requirements for biomaterials is sterilizability, and while various sterilization techniques exist, thermal treatment is one of the most straightforward. Thermal treatment of polymers can induce degradation, transformation and ultimately loss of molecular weight and volatile products; processes that adversely affect the performance of the polymeric biomaterials. In addition, information on the oxidative stability of polymers can be obtained from thermal analysis. The thermal analysis of PLA-*b*-PEG is thus of great interest from both an application and technical perspective. Thermogravimetric analysis (TGA) in air is a classical technique used to evaluate both the thermal and the oxidative stability of polymers. The TGA profiles of copolymers **1**-**8** consisted of three distinct degradation steps corresponding to the thermal degradation of the PLA block, the thermal degradation of the PEG block and the volatilization of the PEG block, respectively. The two-step thermal degradation profile of the

PEG block correlates well with the degradation and volatilization steps reported for linear PEG TGA analysis in air.[39] An overlay of the profiles of four representative copolymers of different tacticities is shown in Figure 2.

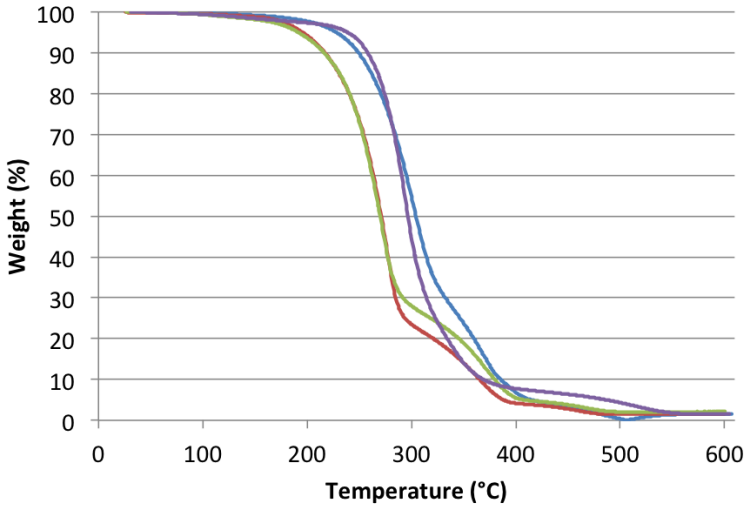

Figure 2. TGA profiles of representative PLA-*b*-PEG copolymers. Red, isotactic copolymer **1**; green, atactic copolymer **6**; blue, isotactic stereoblock copolymer **7**; purple, heterotactic copolymer **8**.

While the effect of stereocontrol on the thermal stability of PLA has been previously reported,[20,21] no significant effect was observed in these block copolymers. The long PEG block used in this study may have masked the effect of tacticity on the thermal stability of these copolymers, with PEG degradation commencing at 173°C. Interestingly, the Al-series of copolymers were more thermally stable than the Sn-series (Figure 2, Table 2), in agreement with literature reports comparing thermal stability of linear PLA homopolymers synthesized using tin- and aluminum-based catalysts.[40] This difference in stability may be justified by the relative proclivity of the catalysts to promote transesterification. As the mechanism of thermal degradation of PLA proceeds via random main chain scission and unzipping depolymerization that includes intramolecular and intermolecular transesterification,[41] hydroxy and carboxy-terminated PLA synthesized using **A** may favor transesterification,[40] and thus thermal degradation could be promoted at a lower temperature via latent catalyst residues. No transesterification has been reported with the salan and salen catalysts,[42] suggesting that residual catalyst may play an important role in polymer stability. In spite of these differences, the thermal stability of the copolymers is well-suited for both thermal sterilization and processing with only 5% weight loss before degradation onset at ≥177°C.

Table 2. TGA[a], DSC[b] and p-XRD[c] Data for PLA-*b*-PEG Copolymers

Entry	5% (°C)[d]	Onset (°C)[e]	50%(°C)[f]	T_g (°C)	T_m (°C)	T_c (°C)	ΔH_m (J/g)	X_c (%)
1	196	240	271	13	41, 150[g]	-	36, 28[h]	29
2	177	220	263	-39	38, 103[g]	-	24, 2[h]	23
3	185	219	265	-43	34	9	52	22
4	188	239	272	-44	29	14	41	22
5	187	218	266	-41	31	17	40	24
6	192	236	270	-43	40	16	41	24
7	227	260	304	-41	39, 133[g]	-	1, 4[h]	24
8	239	267	297	-30	34	-	-	20

[a] TGA conducted in air at a heating rate of 10 °C/min. [b] DSC conducted under N_2 at a heating and cooling rates of 5 °C/min. [c] p-XRD conducted at $\lambda = 1.542$ Å and $K = 0.9$ [d] Temperature at 5% weight loss. [e] Onset temperature at intense decomposition. [f] Temperature at 50% weight loss. [g] T_m of the PLA block. [h] ΔH_m of PLA block.

The T_g, T_m and T_c of the copolymers were measured under nitrogen using DSC. While literature reports indicate that the T_g of PEG (M_n = 2000 Da) is -60°C,[43] PLA exhibits a T_g of 50°C to 70°C depending on microstructural features.[44] All copolymers in this study exhibited a single T_g interpolated between that of homopolymers of PEG and PLA, implying an absence of phase separation between blocks in the solid state, consistent with a similar observation on a related copolymer.[30] Apart from the relatively high T_g of the isotactic stereopure copolymer **1** (13 °C) and heterotactic copolymer **8** (-30 °C), with stereoregular PLA blocks, the other copolymers exhibited similar T_g values that ranged between -44 °C and -39 °C. The lack of effect of tacticity on the glass transition is likely due to the miscibility of the amorphous regions of both blocks in the copolymer. Overall, the glass transition temperatures of the copolymers were all lower than body temperature making the materials suitable as potential soft tissue fillers. Copolymers with higher P_m (**1**, P_m = 100%; **2**, P_m = 84%; and **7**, P_m = 80%) exhibited two distinct T_m transitions for the melting transitions of the PEG and PLA blocks, the second arising from the semi-crystalline PLA block. The amorphous atactic and heterotactic PLA-*b*-PEG materials showed only a single T_m transition. The PLA block of the isotactic stereoblock **7** had a T_m that was significantly higher than that of the predominantly isotactic **2** of similar P_m, suggesting increased crystallinity for the stereoblock material. The ΔH_m of the PLA block (Table 2) also indicates that copolymer **7** was slightly more crystalline than copolymer **2**. Clearly, isotactic stereopure copolymer **1** exhibited the highest degree of crystallinity among the copolymers as shown from the ΔH_m and X_c (Table 2). Regrettably, p-XRD did not reveal any significant difference in the X_c of copolymers **2**-**8**. This suggests that tacticity can play a significant role in determining whether a polymer exhibits semi-crystalline or amorphous features, but not further crystallinity tuning. Further, as shown in the DSC profiles in Figures 3a-d and Figures S2a-d (see supporting information), the thermal transitions of the Sn-series of copolymers were more marked than those of the Al-series. Interaction between residual catalyst and polymer may affect thermal properties of these aliphatic polyesters, as supported by reports[40] that tin(II) and aluminum(III) interact differently with polyester chains.

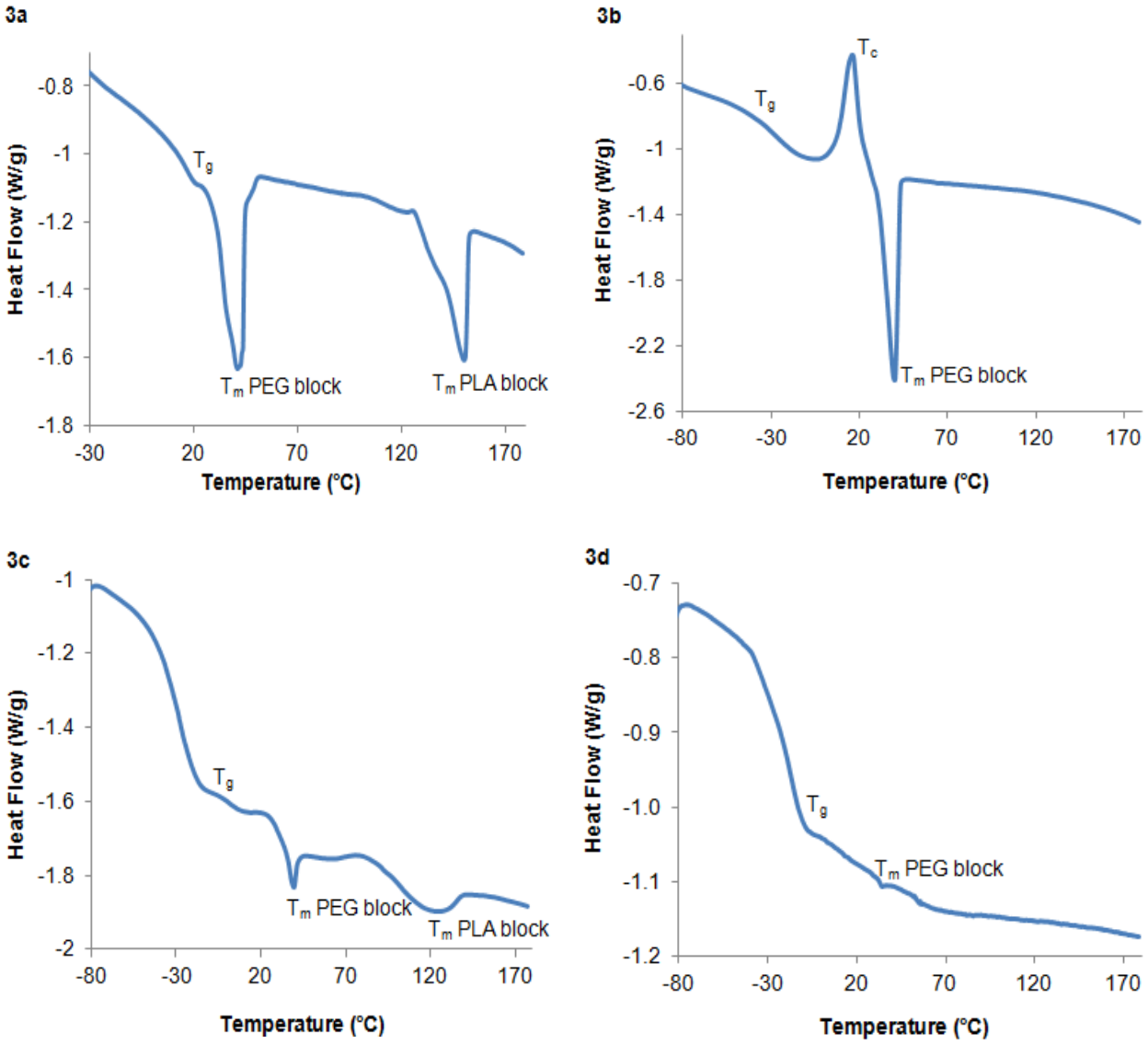

Figures 3a-d. DSC thermograms for representative PLA-*b*-PEG copolymers. 3a, isotactic stereopure copolymer **1**; 3b, atactic copolymer **6**; 3c, isotactic stereoblock copolymer **7**; 3d, heterotactic copolymer **8**.

Hydrolytic degradation of PLA block. While the PLA block of the copolymers is readily hydrolytically degradable, the PEG is inert under standard conditions. The microstructural features of poly(lactic acid)s, as well as the nature of the degradation media, control the rate of the degradation process, including polymer erosion.[45] While degradation involves bond scission to form oligomers, and ultimately monomers, erosion involves the depletion of the material due to dissolution of the degradation products; most often, the latter process follows the former.[46] Under alkaline conditions, as used in this study, degradation of PLA homopolymers proceeds via intramolecular transesterification to form lactic acid.[47] In this work, TBD-promoted degradation readily produces lactic acid as evidenced by ^{1}H NMR spectra of the degraded pellets showing prominent signals at δ 4.3 ppm corresponding to the methine proton of lactic acid (CH_{LA}) after one week (Figure 4). For the Sn-series of copolymers an increase in the intensity of CH_{LA} signal correlated negatively with P_m, suggesting that increased isotactic enchainment inhibits hydrolytic degradation. The heterotactic copolymer **8** degraded more completely than the other copolymers, potentially due to the consistency of

reactive meso linkages in the backbone; the signal at δ 5.2 ppm that corresponded to the methine proton of PLA (CH_{PLA}) was virtually absent (< 1%) after one week.

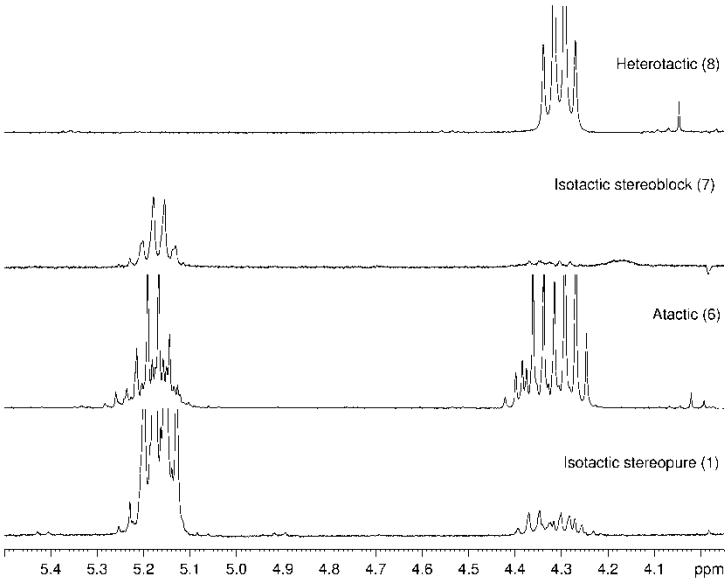

Figure 4. ^{1}H NMR spectra of TBD-degraded copolymers after one week in $CDCl_3$.

A pH test of the solution of the degraded copolymers after one week indicated a slightly acidic solution for the Sn-series of copolymers and an alkaline solution for the Al-series, even with equal initial loadings of TBD base. This difference in pH may also account for the enhanced degradation of the heterotactic copolymer **8**, as the degradation of PlLA films in acidic media proceeds slower than in alkaline media,[48] although the nature of the catalyst may also play a role in determining hydrolytic degradation rates.[49,50] Both hypotheses contrast with the fact that degraded isotactic stereoblock copolymer **7**, while alkaline and produced with aluminum catalysts, did not show any enhancement to degradation over polymers with similar P_m, suggesting that the nature of the tactic linkages plays a predominant role. GPC analyses of the degraded copolymers identified short chain oligomers, with M_n changes correlating negatively with P_m and the heterotactic copolymer **8** showing the greatest molecular weight differences, supporting a more complete degradation (Table 3).

Table 3. Change in Molecular Weights,[a] Erosion Times[b] and CMCs of PLA-*b*-PEG copolymers.

Entry	Change in M_n (%)	Erosion Time (min)	CMC (mg/mL)
1	14	208	0.0050
2	39	88	0.0025
3	42	95	0.0008
4	49	30	0.0005
5	58	28	0.0005
6	63	29	0.0005
7	36	98	0.0025
8	78	71	0.0005

[a] Based on M_n obtained from GPC analyses before and after degradation. [b] Based on the visual observation of the time taken for the disintegration of pressed pellet of copolymer

The formation of oligomers and monomers as the degradation agent diffuses into the amorphous regions leads to gradual depletion of the pellets. In our study, the disintegration of the pellet is correlated to its erosion.[20,21] The erosion time of PLA-*b*-PEG copolymers correlated positively with P_m, with the isotactic stereopure copolymer **1** (P_m = 100%) depleting over longest time (208 minutes) while the atactic **6** (P_m = 34%) took only 29 minutes to completely deplete (Table 3). While results from ^{1}H NMR and GPC studies suggested that the heterotactic **8** degraded more completely, data from the erosion of the pellets showed that **8** depletes faster than only **1**, **2**, **3** and **7**. This finding implies that while the degradation could be influenced by an interplay of polymerization conditions and microstructural features, the pellet erosion depends on more complex processes such as degradation, swelling, dissolution, and diffusion of oligomers and monomers.[51] Indeed, erosion of the pellets does not necessarily follow chain scission, as the former process can take place with little or no degradation. Notably, isotactic stereoblock copolymer **7** was completely depleted in a comparable time to the stereoregular poly(l-lactic acid) copolymer of similar P_m, **2**, suggesting that tacticity was the major factor in determining erosion times.

Critical Micelle Concentration. The critical micelle concentrations (CMCs) of the copolymers were determined by means of a fluorescence spectroscopy method with pyrene as a probe. Pyrene senses a polar environment in an aqueous solution in the absence of micelles (i.e. below a CMC). As micelles are formed, pyrene preferentially partitions towards the hydrophobic core of the micelles, transitioning to a non-polar environment. While a number of changes are associated with the partitioning of pyrene between the two phases, we examined the increase in the fluoresence intensity of the first vibrational band (I_1) and a change in the vibrational fine structure of the emission spectra, which is related to I_1/I_3.[32-34] The intensity of the first vibrational band was plotted against the copolymer concentration to obtain the CMCs with the concentration that corresponds to a sharp increase in intensity indicating onset of micellization (Figure 5 and Figures S3a-d in supporting information). At a low copolymer concentration, negligible change in intensity was observed as the pyrene was preferentially partitioned in the polar water phase. As the concentration increases, the intensity increases significantly as sequestration of the pyrene within the hydrophobic core takes place, suggesting the onset of micellization. The CMCs for the copolymers are given in Table 3.

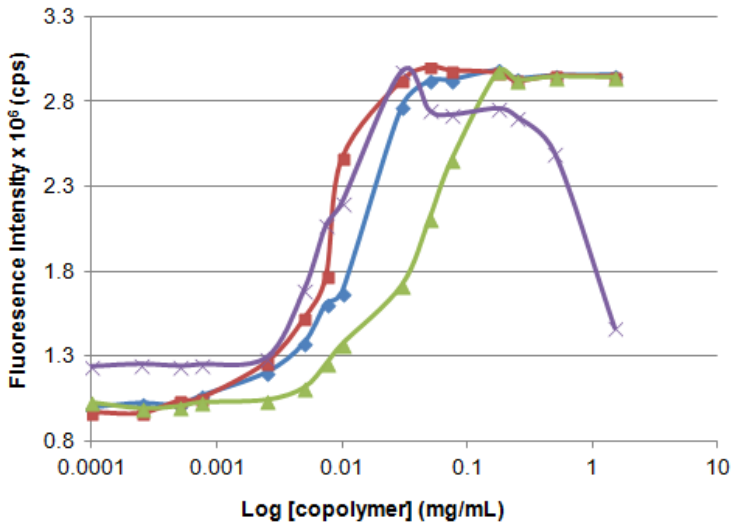

Figure 5. Plot of fluorescence intensity as a function of [copolymer] for representative copolymers. Green triangle, isotactic stereopure copolymer **1**, red square, atactic copolymer **6**; purple cross, isotactic stereoblock **7**; blue diamond, heterotactic **8**.

Tacticity is a major determining factor for the CMCs of the copolymers. A decrease in CMC correlated positively with a decrease in P_m as highlighted by the isotactic stereoblock copolymer **7** (P_m = 80%) and the predominantly isotactic copolymer **2** (P_m = 84%) exhibiting the same CMC value. The role of tacticity on micellization of this class of amphiphilic copolymers may be linked to the semi-crystalline nature of isotactic PLA blocks, as the crystallinity of the hydrophobic core has previously been reported to influence the CMCs of poly(ethylene glycol)-*block*-poly(caprolactone-*co*-lactic acid) copolymers.[52] This is further supported by amorphous, heterotactic copolymer **8** having a similar CMC to the predominately atactic, amorphous copolymers **3**-**6**. The dependence of CMC on tacticity bias implies that micellar stability can be tuned through control of tacticity. As the isotactic copolymers **1** and **2** and the isotactic stereoblock **7** had relatively long semi-crystalline segments, correlating with their high P_m, their high CMCs could be attributed to the tightly packed structure of their isotactic hydrophobic core, which may restrict pyrene partitioning into the core. In a crystalline core, the chain packing is ordered and may favor more copolymers self-assembling into one micelle to reduce the surface tension in the hydrophobic core-solvent interface. As the micelles become larger, the free energy of micellization increases due to increased repulsion between the dense corona chains, thereby limiting the growth of the micelles.

Interestingly, Figure 5 also shows unprecedented behavior for the isotactic stereoblock copolymer **7**, which seems to release the incorporated pyrene into the aqueous phase above 0.03 mg/mL. This unexpected finding is reproducible and pronounced, and suggests that either the micellar core of the isotactic stereoblock PLA-*b*-PEG was disrupted or pyrene fluoresence was suppressed at high micelle concentration. The plot of the quotient of first and third vibrational band intensities (I_1/I_3) as a function of copolymer concentration also confirms that less pyrene was incorporated into the micellar core of the isotactic stereoblock copolymer **7** at high concentration. A plot of representative copolymers with PLA blocks of different tacticity biases is shown in Figure 6. This behavior could not be attributed solely to the crystallinity of the hydrophobic core as isotactic stereopure copolymer **1** had the highest degree of crystallinity than the isotactic stereoblock **7** (ΔH_m and X_c, Table 2) and, in fact, little differences were noted between the crystallinity of all samples with an isotactic bias. To further confirm this, we investigated the micellization of a copolymer with a stereocomplex (sc)[38,54,55] PLA core with pyrene probe, blending stereopure poly(l-lactic acid) and poly(d-lactic acid) prior to micellization. The desired sc-PLA-*b*-PEG was prepared via room temperature mixing of equal volumes of 2 mg/mL solutions of isotactic stereopure P(l-LA)-*b*-PEG (**1**) and P(d-LA)-*b*-PEG (**9**) and allowing the mixture to stand overnight.[56] The plot of I_1/I_3 as a function of the concentration of the resulting copolymer solution with sc-PLA (**1**:**9**) was similar to that of isotactic stereopure copolymers **1** and **9**, but differed significantly from that of the isotactic stereoblock copolymer **7** (Figure 7).

Table 4. Microstructural and polymerization data of PLA-*b*-PEG copolymers[a]

Entry	Conversion[b] (%)	Catalyst	Monomer (l:*rac*:d)	$M_{n,th}$	$M_{n,GPC}$[c]	M_w[c]	$M_{n,NMR}$[d]	PDI[c]	P_m[e]
9	98	**A**	0:0:100	5248	4770	6310	5200	1.32	1.00
10	98	**D**	0:100:0	5248	4870	5400	5390	1.11	0.88

[a] Polymerization carried out at 70 °C in 5 mL toluene with monomer:initiator:catalyst ratio of 23:1:1. [b] Conversion obtained from ^{1}H NMR spectra. [c] M_n, M_w and PDI obtained from GPC analyses. [d] Mn obtained from ^{1}H NMR

spectroscopic analyses [e] P_m, isotactic enchainment in the PLA block obtained from homonuclear decoupled ^{1}H NMR spectra of the methine proton of the PLA block.

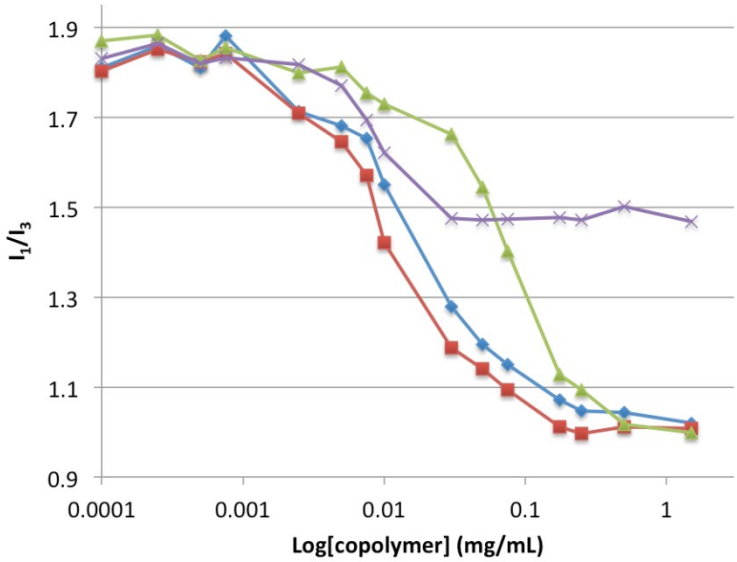

Figure 6. Plot of I_1/I_3 as a function of [copolymer] for representative copolymers. Green triangle, isotactic stereopure copolymer **1**, red square, atactic copolymer **6**; purple cross, isotactic stereoblock copolymer **7**; blue diamond, heterotactic copolymer **8**.

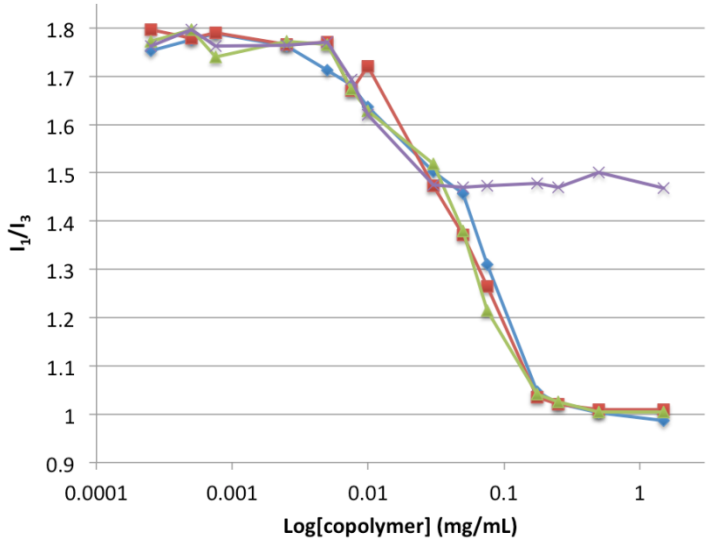

Figure 7. Plot of I_1/I_3 as a function of [copolymer] for different tacticities. Red square, isotactic stereopure **1**; purple cross, isotactic stereoblock **7**; blue diamond, isotactic stereopure **9**; green triangle, isotactic stereocomplex PLA-*b*-PEG **1:9**.

The results in Figure 7 imply that the unique behavior exhibited by isotactic stereoblock **7** was not due to high crystallinity or a high isotactic bias. Subsequent to this finding, we investigated the micellization of isotactic stereoblock copolymers **10** on the assumption that the reduced pyrene uptake at high concentration may be due to the aluminum salen catalyst and the unique long stereoblocks it forms. Copolymer **10** was prepared using a designed aluminum salen catalyst (**D**, Figure 1) substituted with bulky adamantyl groups[29] to afford a higher isotacticity bias (P_m = 90%). Plots of I_1/I_3 and I_1 as a function of copolymer concentration (Figures 8a and b) indicate that the isotactic stereoblock copolymers **7** and **10** and show similar micellization properties in the presence of pyrene probe**.** While the CMCs of the isotactic stereoblock copolymers (**7**, CMC = 0.0025 mg/mL; **10**, CMC = 0.005 mg/mL) correlate positively with the P_m, as observed with the other copolymers, both copolymers show a pronounced decrease in I_1 at 0.03 mg/mL. We initially attributed this transition to either a migration of pyrene from the hydrophobic core to the aqueous phase through a change or disintergration in micelle morphorlogy or the suppression of pyrene fluoresence by the aluminum salen catalyst. The suppression of the pyrene probe at high copolymer concentration was plausible, as the salen ligands are known fluorophores that are being explored as chemosensors.[56,57] However, mixtures of ligand, aluminum complex and/or pyrene in non-polar solvents did not exhibit fluorescence suppression, suggesting that micellar degradation may be the cause of the fluorescence quenching. Further, studies on the morphology of these copolymer micelles is ongoing but beyond the scope of this study.

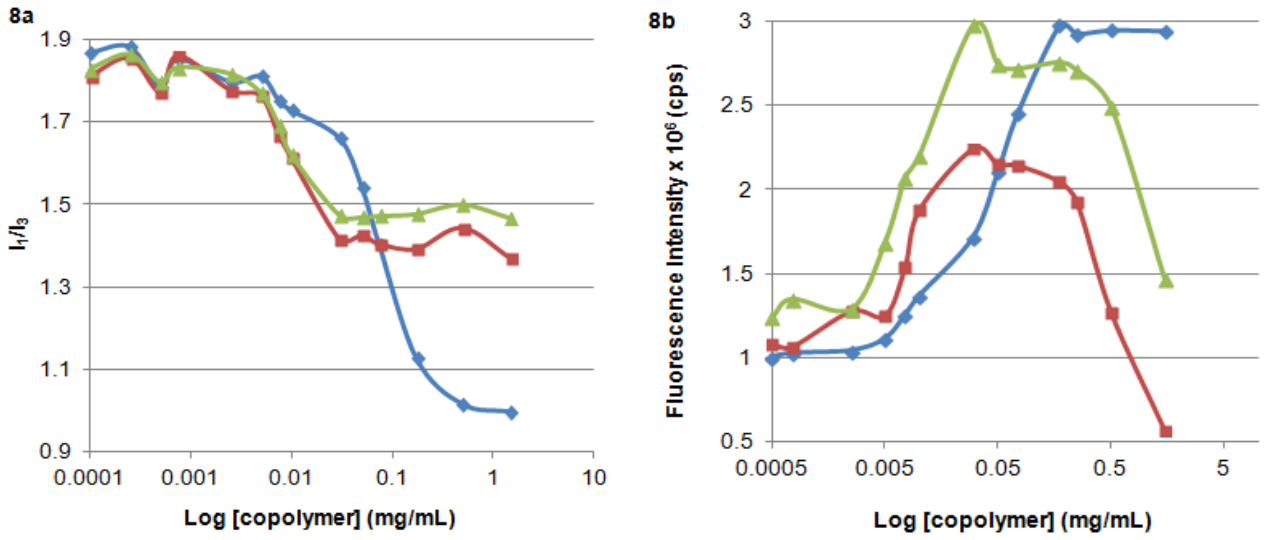

Figure 8. Plot of a, I_1/I_3; and b, fluorescence intensity as a function of [copolymer] for copolymers of varying isotactic block length. Blue diamond, isotactic stereopure **1**; green triangle, isotactic stereoblock **7**; red square, isotactic stereoblock **10**.

Conclusion

The thermal, degradation and micellization properties of PLA-*b*-PEG copolymers were studied as a function of tacticity. In the series of copolymers investigated, the long chain of the PEG macroinitiator masked the effect of tacticity on thermal properties. Catalyst residues were found to influence the thermal stability of the copolymers,

increasing the stability of the Al-series of copolymers. Copolymers that had low P_m or heterotactic PLA blocks degraded and depleted faster than those that were predominantly isotactic. While differences in polymerization conditions affected the degradation of the PLA block, tacticity was found to be the major factor influencing copolymer erosion under the conditions used in this study.

We have also shown that low P_m and heterotacticity in the PLA block of the copolymers correlated positively with low CMC and higher micellar stability, an important finding as micellar *in vivo* stability can thus be controlled by modification of tacticity of the PLA block. The micellization of aluminum salen-catalyzed PLA-*b*-PEG copolymers in the presence of a pyrene probe was different to that of the tin-catalyzed- and aluminum salan-catalyzed copolymers. Either a disintegration of the micelles or suppression of pyrene fluorescence could be responsible for this behavior. Currently, we are investigating the photophysical properties and self-assembly of several aluminum salen-catalyzed PLA-*b*-PEG copolymers with different isotactic enchainments to provide a complete and conclusive picture of this unique behavior.

References

[1] Yu, Y.; Pang, Z.; Lu, W.; Yin, Q.; Gao, H.; Jiang, X. *Pharm. Res.* **2012***, 29,* 83-96.

[2] Graf, N.; Bielenberg, D. R.; Kolishetti, N.; Muus, C.; Banyard, J.; Farokhzad, O. C.; Lippard, S. J. *ACS Nano* **2012***, 6,* 4530-4539.

[3] Tong, R.; Cheng, J. *Macromolecules* **2012***, 45,* 2225-2232.

[4] Li, Y.; Fukushima, K.; Coady, D. J.; Engler, A. C.; Liu, S.; Huang, Y.; Cho, J. S.; Guo, Y.; Miller, L. S.; Tan, J. P. K.; Ee, P. U. R.; Fan, W.; Yang, Y. Y.; Hedrick, J. L. *Angew. Chem. Int. Ed.* **2013**, *52*, 674-678

[5] Sundararaman, A.; Stephan, T.; Grubbs, R. B. *J. Am. Chem. Soc.* **2008***, 130,* 12264-12265.

[6] Qiu, L. Y.; Bae, Y. H. *Pharm. Res*. **2006**, 23, 1-30.

[7] Kataoka, K.; Harada, A.; Nagasaki, Y. *Adv. Drug Delivery Rev*. **2001**, 41, 113-131

[8] Owen, S. C.; Chan, D. P. Y.; Shoichet, M. S. *Nano Today* **2012***, 7,* 53-65.

[9] Letchford, K.; Burt, H. *Eur. J. Pharm. Biopharm.* **2007***, 65,* 259-269.

[10] Xiong, X.; Falamarzian, A.; Garg, S. M.; Lavasanifar, A. *J. Controlled Release* **2011***, 155,* 248-261.

[11] Yamamoto, Y.; Yasugi, K.; Harada, A.; Nagasaki, Y.; Kataoka, K. *J. Controll. Rel.* **2002***, 82,* 359-371.

[12] Hamidi, M.; Shahbazi, M.; Rostamizadeh, K. *Macromol. Biosci.* **2012***, 12,* 144-164.

[13] Lavasanifar, A.; Samuel, J.; Kwon, G. S. *Colloids Surf. , B* **2001***, 22,* 115-126.

[14] Rosler, A.; Vandermeulen, G. W. M.; Klok, H. *Adv. Drug Delivery Rev.* **2001***, 53,* 95-108.

[15] Kim, S. H.; Tan, J. P. K.; Nederberg, F.; Fukushima, K.; Colson, J.; Yang, C.; Nelson, A.; Yang, Y.; Hedrick, J. L. *Biomaterials* **2010***, 31,* 8063-8071.

[16] Harada, A.; Kataoka, K. *Macromolecules* **1995***, 28,* 5294-5299.

[17] Mahmud, A.; Xiong, X.; Lavasanifar, A. *Macromolecules* **2006***, 39,* 9419-9428.

[18] Jette, K. K.; Law, D.; Schmitt, E. A.; Kwon, G. S. *Pharm. Res.* **2004***, 21,* 1184-1191.

[19] Lavasanifar, A.; Samuel, J.; Sattari, S.; Kwon, G. S. *Pharm. Res.* **2002***, 19,* 418-422.

[20] Cameron, D. J. A.; Shaver, M. P. *J. Polym. Sci., Part A: Polym. Chem.* **2012***, 50,* 1477-1484.

[21] Shaver, M. P.; Cameron, D. J. A. *Biomacromolecules* **2010***, 11,* 3673-3679.

[22] Barz, M. ; Arminan, A. ; Canal, F. ; Wolf, F. ; Koynov, K. ; Frey, H. ; Zentel, R. ; Vicent, M. J. *J. Controlled Release* **2012**, *163,* 63-74.

[23] Mert, O.; Doganci, E.; Erbil, H. Y.; Demir, A. S. *Langmuir* **2008***, 24,* 749-757.

[24] Agrawal, S. K.; Sanabria-DeLong, N.; Jemian, P. R.; Tew, G. N.; Bhatia, S. R. *Langmuir* **2007***, 23,* 5039-5044.

[25] Agrawal, S. K.; Sanabria-DeLong, N.; Coburn, J. M.; Tew, G. N.; Bhatia, S. R. *J. Controlled Release* **2006***, 112,* 64-71.

[26] Saffer, E. M.; Tew, G. N.; Bhatia, S. R. *Curr. Med. Chem.* **2011***, 18,* 5676-5686.

[27] Hormnirun, P.; Marshall, E. L.; Gibson, V. C.; White, A. J. P.; Williams, D. J. *J. Am. Chem. Soc.* **2004***, 126,* 2688-2689.

[28] Hormnirun, P.; Marshall, E. L.; Gibson, V. C.; Pugh, R. I.; White, A. J. P. *Proc. Nat. Acad. Sci.* **2006**, *103*, 15343-15348.

[29] Cross, E. D.; Allan, L. E. N.; Decken, A.; Shaver, M. P. *J. Polym. Sci., Part A: Polym. Chem.* **2013**, *51*, 1137-1146.

[30] Zhao, W.; Wang, Y.; Liu, X.; Chen, X.; Cui, D.; Chen, E. Y. *Chem. Commun.* **2012***, 48,* 6375-6377.

[31] Thakur, K. A. M.; kean, R. T.; Hall, E. S.; Kolstad, J. J.; Lindgren, T. A. *Macromolecules* **1997**, 30, 2422-2428

[32] Mathiowitz, E.; Ron, E.; Mathiowitz, G.; Amato, C.; Langer, R. *Macromolecules* **1990**, 23, 3212-3218

[33] He, G.; Ma, L. L.; Pan, J.; Venkatraman, S. *Int. J. Pharm.* **2007***, 334,* 48-55.

[34] Dominguez, A.; Fernandez, A.; Gonzalez, M.; Iglesias, E.; Montenegro, L. *J. Chem. Educ.* **1997***, 74,* 1227-1231.

[35] Jones, M. -.; Leroux, J. -. *Eur. J. Pharm. Biopharm.* **1999***, 48,* 101-111.

[36] Joung, Y. K.; Lee, J. S.; Park, K. D.; Lee, S-J. *Macromol. Res.* **2008**, 16, 66-69

[37] Thomas, C. M. *Chem. Soc. Rev.* **2010***, 39,* 165-173.

[38] Hirata, M.; Kimura, Y. In *Poly(lactic acid): Synthesis, Structure, Properties, Processing and Applications,* 1st ed.; Auras, R., Lim, L-T., Selke, S.E.M., Tsuji, H. Eds.; John Wiley & Sons, Inc.: Hoboken, NJ, 2010; pp 59-65.

[39] D'Antone, S.; Bignotti, F.; Sartore, L.; D'Amore, A.; Spagnoli, G.; Penco, M. *Polym. Degrad. Stab.* **2001***, 74,* 119-124.

[40] Degee, P.; Dubois, P.; Jerome, R. *Macromol. Chem. Phys.* **1997***, 198,* 1985-1995.

[41] Nishida, H. In *Poly(lactic acid): Synthesis, Structure, Properties, Processing and Applications,* 1st ed.; Auras, R., Lim, L-T., Selke, S.E.M., Tsuji, H. Eds.; John Wiley & Sons, Inc.: Hoboken, NJ, 2010; pp 401-412.

[42] Dechy-Cabaret, O.; Martin-Vaca, B.; Bourissou, D. *Chem. Rev*. **2004**, 104, 6147-6176

[43] Rashkov, I.; Manolova, N.; Li, S. M.; Espartero, J. L.; Vert, M. *Macromolecules* **1996***, 29,* 50-56.

[44] Fambri, L.; Migliaresi, C. In *Poly(lactic acid): Synthesis, Structure, Properties, Processing and Applications,* 1st ed.; Auras, R., Lim, L-T., Selke, S.E.M., Tsuji, H. Eds.; John Wiley & Sons, Inc.: Hoboken, NJ, 2010; pp 113-124.

[45] Tsuji, H. In *Poly(lactic acid): Synthesis, Structure, Properties, Processing and Applications,* 1st ed.; Auras, R., Lim, L-T., Selke, S.E.M., Tsuji, H. Eds.; John Wiley & Sons, Inc.: Hoboken, NJ,2010; pp 345-381.

[46] Albertsson, A-C.; Varma, I. K. *Adv. Polym. Sci.* **2002***, 157,* 1-40.

[47] De Jong, S. J.; Arias, E. R.; Rijkers, D. T. S.; Van Nostrum, C. F.; Kettenes-Van den Bosch, J. J.; Hennink, W. E. *Polymer* **2001***, 42,* 2795-2802.

[48] Tsuji, H.; Nakahara, K. *J. Appl. Polym. Sci.* **2002***, 86,* 186-194.

[49] Schwach, G.; Coudane, J.; Engel, R.; Vert, M. *Biomaterials* **2002***, 23,* 993-1002.

[50] Stefani, M.; Coudane, J.; Vert, M. *Polym. Degrad. Stab.* **2006***, 91,* 2853-2859.

[51] Gopferich, A. *Biomaterials*, **1996**, *17*, 103-114

[52] Zhang, J.; Wang, L.; Wang, H.; Tu, K. *Biomacromolecules* **2006***, 7,* 2492-2500.

[53] Agrawal, S. K.; Sanabria-Delong, N.; Tew, G. N.; Bhatia, S. R. *Macromolecules* **2008**, *41*, 1774-1784.

[54] Chen, L.; Xie, Z.; Hu, J.; Chen, X.; Jing, X. *J. Nanopart. Res.* **2007**, *9*, 777-785.

[55] Kersey, F. R.; Zhang, G.; Palmer, G. M.; Dewhirst, M. W.; Fraser, C. L. *ACS Nano* **2010**, *4*, 4989-4996.

[56] Whiteoak, C. J.; Salassa, G.; Weij, A. W. *Chem. Soc. Rev.* **2012**, *41*, 622-631.

[57] Li, J.; Wu, Y.; Song, F.; Wei, G.; Cheng, Y.; Zhu, C. *J. Mater. Chem*. **2012**, *22*, 478-482.